What can we learn from giant resonances in light nuclei?

I T Usman[1], J Carter[1], L M Donaldson[1,2], P Adsley[1,2], A Bahini[1,2], R Neveling[2], M Jingo[1,3], C O Kureba[1,4], M B Latif[1,5], S D Olorunfunmi[1,6], E Sideras-Haddad[1] F D Smit[2], N Y Kheswa[2], P von Neumann-Cosel[7], A Richter[7], R Roth[7], V Yu Ponomarev[7], Papakonstantinou[8], E Litvinova[9], N Arsenyev[10], V O Nesterenko[10], A Severyukhin[10], and H Fujita[11]

[1] School of Physics, University of the Witwatersrand, Johannesburg 2050, South Africa
[2] SSC Laboratory, iThemba LABS, Faure, Cape Town 7131, South Africa
[3] School of Clinical Medicine, University of the Witwatersrand, Johannesburg 2000, South Africa
[4] Department of Physics and Astronomy, Botswana International University of Science and Technology, Palapye, Botswana
[5] Center for Energy Research and Development, Obafemi Awolowo University, Ile-Ife, 220005 Nigeria
[6] Department of Physics and Engineering Physics, Obafemi Awolowo University, Ile-Ife, 220005 Nigeria
[7] Institut für Kernphysik, Technische Universität Darmstadt, D-64289, Darmstadt, Germany
[8] Rare Isotope Science Project, Institute for Basic Science, Daejeon 305 - 811, South Korea
[9] Department of Physics, Western Michigan University, Kalamazoo MI 49008-5252, USA
[10] Bogoliubov Laboratory of Theoretical Physics, Joint Institute for Nuclear Research, 141980 Dubna, Moscow region, Russia
[11] Research Center for Nuclear Physics, Osaka University, Ibaraki, Osaka 650-0047, Japan

E-mail: iyabo.usman@wits.ac.za

Abstract. Extensive experimental investigations into understanding the fine structure of giant resonances in nuclei across the periodic table have been carried out in recent years using the state-of-the-art K600 magnetic spectrometer of iThemba LABS, Cape Town, South Africa. Based on the established results in comparison to various theoretical calculations, it has been found that the fine structure observed in different giant resonances, namely Isoscalar Giant Quadrupole Resonance (ISGQR), Isovector Giant Dipole Resonance (IVGDR) and Isoscalar Giant Monopole Resonance (ISGMR), in light nuclei such as ^{40}Ca, ^{28}Si and ^{27}Al is dominated by Landau damping although signatures for the role of the spreading width are also found. In this report, characteristic energy scales extracted in light nuclei are compared with the state-of-the-art theoretical calculations, while the fine structures results obtained are compared using semblance analysis to search for possible signatures of common fragmentation patterns induced by Landau damping and coupling to 2p-2h states obtained from different giant resonances.

1. Introduction

Experimental and theoretical studies of the giant resonances provide insights into the main mechanism leading to the fine structure phenomena. Collective modes are treated as smallamplitude vibrations around the ground state. Major processes that contribute to the excitation and decay of giant resonances include Landau damping, escape width and spreading width. Meanwhile, the only way to understand the origin and physical nature of different scales is by comparison of experimentally observed values with model predictions. In a novel application of the wavelet analysis technique, it was shown that the energy scales extracted from experimental spectra could be related to those determined from microscopic model calculations including 2p-2h degrees-of-freedom. In the recent years, using the K600 magnetic spectrometer of iThemba LABS, most of these contributions have been observed from the range of giant resonances studied in nuclei across the periodic table. Identification of energy scales in high energy-resolution alpha and proton inelastic scattering exciting giant resonances in nuclei over a wide range has been studied in Refs. [1, 2, 3, 4, 5, 6, 7, 8, 9, 10, 11]. It is already known that giant resonances in low-mass nuclei are highly fragmented from the investigations using a variety of nuclear probes and theoretical models. Hence, it is of interest to compare the energy scales extracted from different giant resonances region for each nucleus. To accomplish this, quantitative analyses were carried on ^{40}Ca, ^{28}Si and ^{27}Al for ISGQR, ISGMR and IVGDR data using the Semblance Analysis technique in order to extract information about the level of correlation that exists between these experimental data.

2. Experiments

The fine structure of the ISGQR, ISGMR and IVGDR have been investigated in ^{40}Ca, ^{28}Si and ^{27}Al using the Separated-Sector Cyclotron (SSC) of iThemba LABS, which delivers high quality proton and alpha beams at and close to 200 MeV to the K600 magnetic spectrometer scattering chamber. Full detailed of the experimetal setups including dispersion matching techniques are given in Refs. [3, 4, 5, 10, 11, 12, 13]. Table 1 shows more information about each of the experiments as well as targets and energy resolution achieved using the K600 magnetic spectrometer at iThemba LABS.

Table 1. High energy-resolution Giant Resonances experiments at iThemba LABS.

Resonances	E_{Lab} (MeV)	Targets	Energy resolution (keV)
ISGQR (p,p′)	200	^{12}C, ^{27}Al, ^{28}Si, ^{40}Ca (Refs. [3, 4, 5])	25 - 38
		^{58}Ni, ^{89}Y, ^{90}Zr, ^{120}Sn, ^{166}Er, ^{208}Pb (Refs. [1, 2])	35 - 50
		^{142,144,148,150}Nd (Ref. [7])	25 - 35
ISGMR (α,α')	196	^{24}Mg, ^{28}Si, ^{58}Ni, ^{90}Zr, ^{120}Sn, ^{208}Pb (Ref. [11])	60 - 80
		^{40,42,44,48}Ca (Ref. [10])	60 – 80
IVGDR (p,p′)	200	^{27}Al, ^{56}Fe, ^{58}Ni, ^{208}Pb (Ref [6])	35 – 50
		^{40,42,44,48}Ca (Refs. [9, 12])	30 – 40
		^{142,144,148,150}Nd, ^{152}Sm (Refs. [8, 14])	40 – 45

3. Semblance Analysis and discussion of results

A wavelet transform is defined as a convolution of the original energy spectrum $\sigma(E)$ multiplied by a scaled, shifted version of a wavelet function Ψ. The coefficients $C(E_{\mathrm{x}}, \delta E)$ of the wavelet transform are obtained as

$$C(E_x, \delta E) = \frac{1}{\sqrt{\delta E}} \int \sigma(E)\, \Psi(\frac{E_x - E}{\delta E}) dE, \tag{1}$$

where δE is the scale and E_x is the position along the energy scale, respectively.

The parameters, excitation energy, E_x, and scale, δE, can be varied continuously (Continuous Wavelet Transform, CWT) or in discrete steps j, where $\delta E = 2^j$, $j = 1, 2, 3, \ldots$, and $E_x = \delta E$. A variety of wavelets provide a set of tools for performing many different tasks. The choice of a particular wavelet is based on its mathematical properties [15, 16] amongst which are moments, compact support and the regularity of a signal (the number of times that it is continuously differentiable). Complex wavelets produce a complex wavelet transform, allowing the phase of the result to be examined. The choice of a mother wavelet is motivated by the type of spectrum being analyzed. The Morlet mother wavelet used in this analysis is derived by taking a periodic wave and localizing it with a Gaussian envelope

$$\Psi(x) = \frac{1}{\pi^{1/4}} \exp(ikx) \exp\left(-\frac{x^2}{2}\right). \tag{2}$$

Here, the parameter k weighs the resolution in scales *versus* the resolution in localization. A value of $k = 5$ was chosen in the present work.

Quantitative analyses were carried on the ^{40}Ca, ^{28}Si and ^{27}Al data using Semblance Analysis technique in order to extract information about the level of correlation that exists between the experimental giant resonances for each nuclide. Semblance Analysis is a technique used to determine the degree of correlation (both positive and negative) between two data sets, which in the present case is a function of both energy scale and excitation energy. The semblance can take on values between -1 and $+1$. A value of $+1$ implies perfect correlation, 0 implies no correlation, and -1 implies perfect anticorrelation. However, the disadvantage of lack of amplitude information leads to the further use of the Dot product. A Dot product is equivalent to the vector Dot product of the complex wavelet coefficients at each point in scale and excitation energy [17]. This was considered a better option because it combines the phase information of Semblance with the amplitude information of the Continuous Wavelet Transform (CWT) coefficients in order to emphasise the larger amplitude components of the data sets. Extensive details of the complex Morlet wavelet analysis technique using the CWT coefficients as applied to the analysis of fine structure in high energy-resolution giant resonances investigations can be found in Refs. [7, 6, 12, 14]. In a nutshell, the wavelet-based semblance S is given as

$$S = \cos^n(\theta), \tag{3}$$

where n is an odd integer greater than zero, θ is the local phase which can range between $-\pi$ and $+\pi$ given by

$$\theta = \tan^{-1}(\Im(CWT_{1,2})/\Re(CWT_{1,2})) \tag{4}$$

and the cross-wavelet transform

$$CWT_{1,2} = CWT_1.CWT_2^*, \tag{5}$$

where $CWT_{1,2}$ is a complex quantity with CWT_1 as the continuous wavelet transform of dataset 1, and CWT_2 as the continuous wavelet transform of dataset 2. The vector dot-product D of the two complex wavelet vectors can then be written as

$$D = \cos^n(\theta) \mid CWT_{1,2} \mid, \tag{6}$$

respectively. The CWT was applied to the excitation energy region of the giant resonances in the spectra with a Complex Morlet mother wavelet. By plotting the real part of the complex coefficients on a two-dimensional plot of scale *versus* excitation energy, the positions of the structures within the original energy spectrum can be identified as indicated in the second and fourth panels down of the figures below. It is important to note that the present work only shows the correllations between ISGQR and ISGMR, and IVGDR and ISGMR experimental data for ^{40}Ca, ISGQR and ISGMR for ^{28}Si, and IVGDR and ISGQR for ^{27}Al. Shown in Fig. 1 below are the results obtained for Semblance and Dot product analysis of both ISGQR and ISGMR in ^{40}Ca while Fig. 2 shows the same for IVGDR and ISGMR, for ^{40}Ca. Using the same approach, Fig. 3 represents the results of ISGQR and ISGMR in ^{28}Si, and Fig. 4 shows the same for IVGDR and ISGQR in ^{27}Al, respectively.

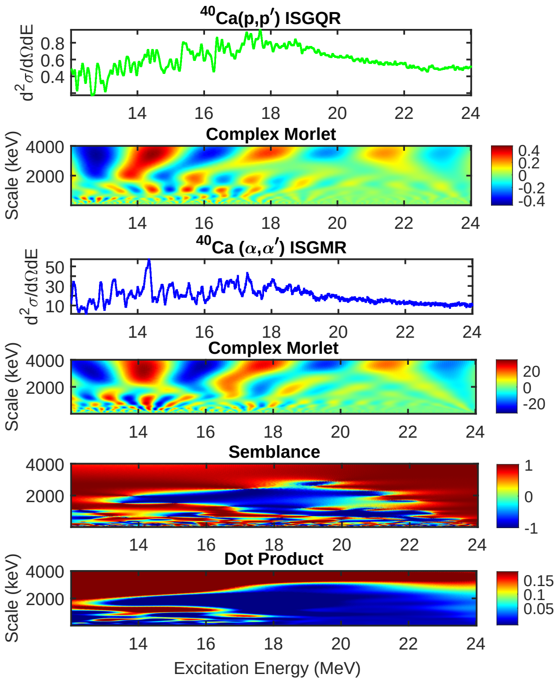

Figure 1. Semblance and Dot product analysis of ISGQR and ISGMR experimental data for ^{40}Ca.

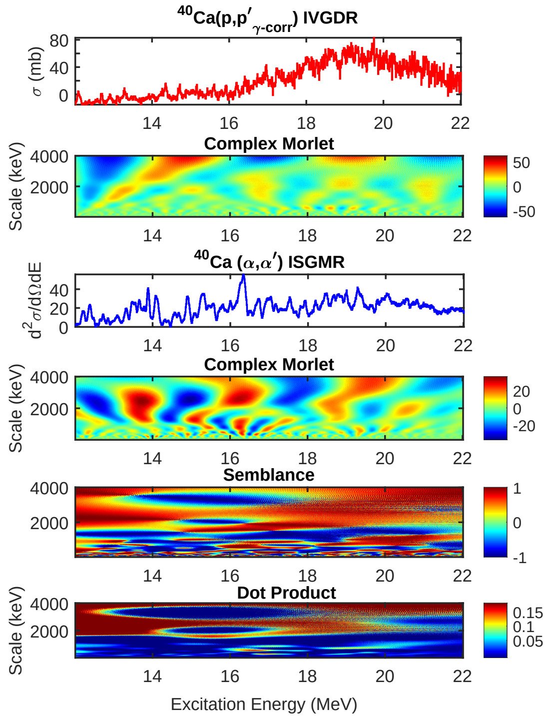

Figure 2. Semblance and Dot product analysis of IVGDR and ISGMR experimental data for ^{40}Ca.

The quantitative correspondence between the three giant resonances can be observed in these figures. There exists a positive correlation of a broad red band in both the Semblance and Dot product results which span across the entire excitation energy range at characteristic scales between 2.0 MeV and 4.0 MeV running through the whole excitation energy region. The Dot product at the bottom of both figures emphasises those regions where both the experimental data has significant strength. In the case of ^{28}Si, only scales between 500 keV and 2000 keV were positively correlated between the ISGQR and ISGMR resonances while most of the anti-correlated region were observed at higher scales and higher excitation energy regions. It can be observed from the figures that positive correlations achieved for the gross width of the resonances for ISGMR, ISGQR and IVGDR in all nuclei with scales above 2000 keV except for ^{27}Al, an odd-even nucleus, which can be related to the shift in the centroid energies between ISGQR and IVGDR due to the restricted configuration available in the extreme single-particle shell model.

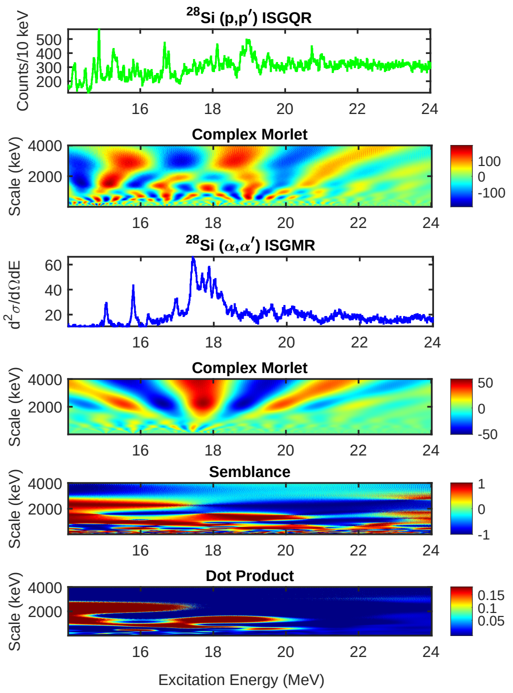

Figure 3. Same as Fig. 1 but for ^{28}Si.

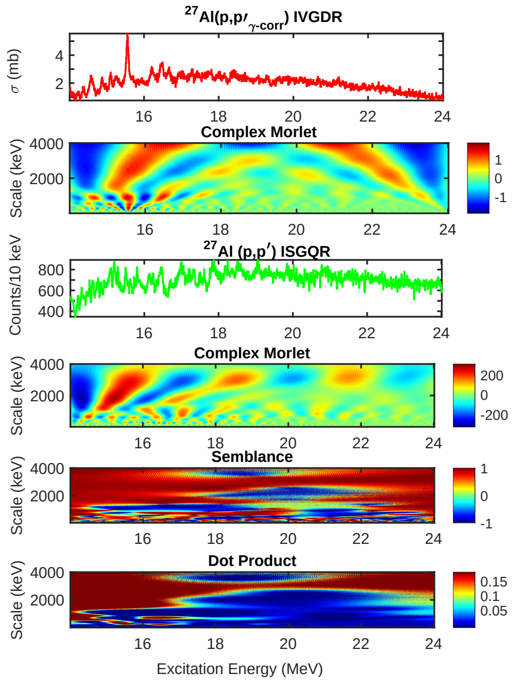

Figure 4. Same as Fig. 2 but for IVGDR and ISGQR experimental data for ^{27}Al.

Hence, the present qualitative results underline the relevance of studies of the fine structure of giant resonances as a tool for an improved understanding of collective modes and their decay. At the same time, the role of Landau fragmentation, escape width and spreading width associated with the damping of the giant resonances in light nuclei have been shown to be significant, based on the established theoretical calculations (see References).

References

[1] Shevchenko A *et al.* 2004 *Phys. Rev. Lett.* **93** 122501
[2] Shevchenko A *et al.* 2008 *Phys. Rev. C* **77** 024302
[3] Usman I *et al.* 2011 *Phys. Lett. B* **698** 191
[4] Usman I *et al.* 2011 *Phys. Rev. C* **84** 054322
[5] Usman I *et al.* 2016 *Phys. Rev. C* **94** 024308
[6] Jingo M *et al.* 2018 *Eur. Phys. J. A* **54** 234
[7] Kureba C O *et al.* 2018 *Phys. Lett. B* **779** 269–274
[8] Donaldson L M *et al.* 2018 *Phys. Lett. B* **776** 133–138
[9] Latif M B *et al.* 2019 *Acta Physica Polonica* Vol. **50**
[10] Olorunfunmi S D *et al.* 2022 *Phys. Rev. C* **105** 054319
[11] Bahini A *et al.* 2022 *Phys. Rev. C* **105** 024311
[12] Carter J *et al.* 2022 *Phys. Lett. B* **833** 137374
[13] Neveling R *et al.* 2012 *Nucl. Instrum. Methods Phys. Res. A* **662** 101
[14] Donaldson L M *et al.* 2020 *Phys. Rev C* **102** 064327
[15] The Mathworks, 2022 *Matlab, The Language of Technical Computing*
[16] 1998 *A Wavelet Tour of Signal Processing*, Academic Press, New York
[17] Cooper G R J and Cowan D R 2008 *Computers and Geosciences* **34** 95